Pedal-Synchronised Closed-Loop Derailleur Control for Low-Cost Automatic Bicycle Retrofit: Design and Protocol

Om Rakshe[1], Pramod Kale[2]
[1,2]*Department of Mechanical Engineering, Vishwakarma Institute of Technology, Pune 411 037, India*

***Abstract*—Manual gear changing demands rider attention, and the low-cost automatic bicycle shifters reported to date typically select gears from wheel speed alone, release shifts at arbitrary points in the pedal stroke and cannot detect a failed shift. This paper presents the design and a pre-specified evaluation protocol for a retrofit controller architecture intended to address these three limitations. The hardware comprises a Hall-effect wheel sensor, a single frame-mounted inertial measurement unit (IMU) and a servo-driven derailleur actuator, with an estimated prototype hardware cost of ₹1,000–1,500. The architecture combines (i) gradient estimation in which wheel-derived longitudinal acceleration is removed before accelerometer and gyroscope data are fused; (ii) cadence and crank-phase inference from the periodic component of frame acceleration, without a crank sensor; (iii) phase-gated shift release, permitted only during sustained pedalling near the crank positions of lowest chain load; and (iv) ratio-based shift verification with bounded, incremental servo-position correction. The controller will be compared with a speed-and-slope baseline running on the same bicycle and hardware, using shift success rate, chain-skip rate, gradient and cadence estimation error, and fault-detection sensitivity and false-alarm rate. No experimental results are reported here. The contribution is the controller architecture, its parameterisation, the baseline definition and the evaluation protocol, specified in sufficient detail for independent replication.**

***Index Terms*—Automatic gear shifting; Cadence inference; Derailleur actuation; Gradient estimation; Inertial sensor; Shift verification**

I. INTRODUCTION

Efficient cycling depends on choosing an appropriate gear, which requires the rider to judge gradient, speed and effort at the same time. Poor choices increase fatigue and drivetrain wear. Automatic transmissions are standard in motor vehicles but remain rare on conventional bicycles because of cost and complexity, although low-cost microcontrollers and inertial sensors now make an inexpensive automatic shifter feasible.

Earlier work has addressed parts of the problem. A fuzzy-logic controller using acceleration, slope and cadence was reported for electric bicycles.[1] Machine-learning shifting with physiological sensing and cloud computing was proposed, but depends on infrastructure unsuited to a standalone retrofit.[2] A moving-cassette electronic shifter used cadence and torque sensors, at the cost of added mass and complexity.[3] An Arduino-based derailleur actuator controlled from wheel speed alone has been described, without terrain sensing or protection against cross-chaining.[4] Data-driven shift control has also been studied for motorcycles, whose dynamics differ from those of human-powered vehicles.[5] Cadence has also been recovered from an inertial unit mounted on the saddle tube using a neural network, which supports the feasibility of off-crank cadence sensing, although that work did not address shift timing or verification.[6] Commercial automatic shifting systems such as Shimano AUTO SHIFT integrate cadence, torque and speed sensing, but are tied to proprietary electronic drivetrain ecosystems and compatible e-bike or Di2 hardware, which limits their use as low-cost retrofit solutions.[7]

These systems show that automatic bicycle shifting can use speed, slope, cadence, torque or physiological inputs. However, among the retrofit-oriented approaches reviewed above, none jointly provides acceleration-compensated gradient estimation, shift release synchronised to a low-load phase of the pedal

stroke, and closed-loop confirmation that the commanded gear has been reached. The simplest retrofit, a speed-and-slope shifter, therefore has three practical weaknesses. First, gradient computed directly from accelerometer axes is corrupted by rider acceleration, pedalling and vibration. Second, a derailleur shifts reliably only when the chain is moving under low load, so shifting at an arbitrary instant or while coasting causes skipping and wear. Third, cable stretch and misalignment make a fixed servo-position table drift, and an open-loop controller cannot detect that a shift has failed.

The objectives of this work are to design a controller that (i) estimates gradient with compensation for rider acceleration; (ii) infers cadence and crank phase without a crank sensor; (iii) releases shifts only at favourable moments of the pedal stroke; and (iv) verifies each shift and corrects the actuator positions automatically, all using inexpensive sensors and a servo-actuated derailleur. Table 1 summarises how the proposed controller differs from the speed-and-slope baseline against which it will be evaluated.

Table 1. Capabilities of the speed-and-slope baseline and the proposed controller

Capability	Speed-and-slope baseline	Proposed controller
Gradient estimation	Accelerometer-only pitch; no compensation for rider acceleration	Acceleration-compensated complementary filter (Eqns 2 and 3)
Pedalling detection	Not used	IMU-derived cadence with confidence score q
Shift timing	Fixed 2 s delay	Phase-gated release near dead-centre crank positions
Shift verification	None	Wheel-to-crank ratio check with servo current monitoring
Servo positions	Fixed table	Bounded incremental self-calibration

Scope of this paper. This is a design and protocol paper. The controller is designed to improve shift success and reduce chain-skip events relative to a speed-and-slope baseline at comparable retrofit cost. These are hypotheses, not findings. No experimental data are presented, and the performance claims will be tested using the protocol in Section 3. Section 2 describes the controller, Section 3 defines the baseline and the evaluation protocol, Section 4 lists the planned outcome measures, and Section 5 discusses design implications and anticipated limitations.

II. MATERIAL AND METHODS: CONTROLLER DESIGN

2.1 Hardware Platform and Cost Basis

The controller (Fig 1; Table 2) uses an Arduino Nano as the processor. Wheel rotation is sensed by a Hall-effect sensor on the fork facing neodymium magnets on the spokes. An MPU6050 inertial unit[8] is fixed to the frame. An HS-755MG metal-gear servo, mounted on a clamp bracket so that the frame is not modified, pulls the derailleur cable. A current sensor on the servo supply measures actuator load, and an SSD1306 display shows speed, gradient and gear. The bicycle has a 3 × 7 drivetrain. The wheel diameter is 0.70 m, giving a circumference C of 2.20 m.

The estimated prototype hardware cost of ₹1,000–1,500 covers the components in Table 2 together with the battery, wiring, enclosure, fasteners and clamp bracket, at prices recorded at the time of purchase. It excludes labour, tools, calibration time and bicycle-specific mechanical adaptation. Because both controllers in the evaluation run on identical hardware (Section 3.1), the comparison isolates the algorithmic contribution. The incremental hardware of the proposed design relative to a wheel-speed-only shifter (the IMU and current sensor) will be costed separately, and an itemised bill of materials will be reported with the evaluation results.

Table 2. Components of the automatic shifting system

Component	Function	Specification
Arduino Nano	Processing and control	ATmega328P, 16 MHz
MPU6050	Acceleration and pitch-rate sensing	3-axis accelerometer and gyroscope; I²C
Hall-effect sensor	Wheel pulses for speed	Digital output; 5 V supply
Neodymium magnets	Trigger sensor on each pass	Spoke-mounted

HS-755MG servo	Derailleur cable actuation	Metal gear; 180° range; 6 V
Current sensor	Servo load monitoring	I²C; on servo supply
SSD1306 display	Rider feedback	128 × 64 pixels; 0.96 in

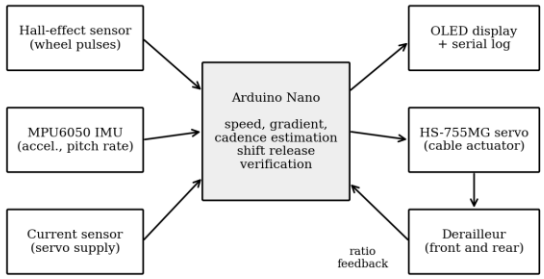


Fig 1. Block diagram of the automatic shifting system

2.2 Wheel Speed Measurement

With m magnets, N pulses counted during a window T and wheel circumference C, the speed v is

$$v = (N/m) \cdot C/T \quad (1)$$

and the wheel rotation frequency is $f_w = N/(mT)$. A window of 1 s is used for the speed that drives gear selection, and pulses are counted by an interrupt on a digital pin, with pulses closer together than a debounce interval rejected. For the acceleration compensation of Section 2.3, speed is instead derived from the interval Δt_p between successive pulses, $v = C/(m\Delta t_p)$, which updates at the pulse rate rather than once per window. One pulse corresponds to a speed step of $C/(mT)$; the number of magnets is therefore chosen at installation so that this step is well below the narrowest speed band in Table 3, and the value used will be reported.

2.3 Gradient Estimation with Acceleration Compensation

Let a_x be the specific force along the forward axis, a_y and a_z the forces along the other axes and a_v the longitudinal acceleration obtained by differentiating the pulse-interval speed of Section 2.2 and low-pass filtering. The group delay of this low-pass filter is matched to that of the accelerometer path, and the residual delay is measured on the bench, because a mismatch would leave a transient error in θ_{acc} during speed changes. The accelerometer pitch with the longitudinal acceleration removed is

$$\theta_{acc} = \text{atan2}(a_x - a_v, \sqrt{(a_y^2 + a_z^2)}) \quad (2)$$

Let ω be the pitch rate from the gyroscope and Δt the sample period. A complementary filter, a standard approach for fusing the accelerometer and gyroscope outputs of low-cost inertial units,[9] gives the pitch estimate θ at sample k:

$$\theta_k = \alpha(\theta_{k-1} + \omega_k \Delta t) + (1 - \alpha)\theta_{acc,k} \quad (3)$$

The coefficient α has an initial value of 0.98 and will be tuned on a bench tilt rig against a digital inclinometer, then frozen before road testing (Table 4). Axis assignment and sign are fixed by a level-ground calibration after mounting. Terrain is classified as uphill ($\theta > 10°$), flat ($-5°$ to $10°$) or downhill ($\theta < -5°$), with hysteresis around each threshold to prevent chatter. These thresholds correspond to road grades of about +17.6% and −8.7%, which are steep relative to typical road climbs. They are therefore provisional: the distribution of gradients on the planned test route will be measured in the pilot, and the thresholds will be revised so that uphill and downhill operation each occupy a meaningful share of riding, then frozen (Table 4).

2.4 Cadence Inference from a Single Inertial Unit

Pedalling excites a periodic component in frame acceleration at the cadence frequency. The vertical-axis signal is sampled at a rate above the control-loop rate, band-pass filtered between 0.5 and 2.0 Hz (30–120 rev min⁻¹), and the dominant frequency f_c is estimated over a sliding window of 4 s. A confidence score q is defined as the ratio of the power at the dominant peak to the total power in the band. If q falls below a threshold q_{min} the rider is classified as not pedalling and cadence-dependent functions are suspended.

To fit the 2 KB of RAM of the processor, the IMU is sampled at 50 Hz (a design value) into a 4 s buffer of 200 samples, about 400 bytes at 16 bits. The dominant frequency is found with a Goertzel filter bank over 30–120 rev min⁻¹ with interpolation about the peak, which avoids a full FFT. Loop timing and memory use will be profiled and reported. If the 100ms loops cannot be met, a faster 32-bit microcontroller will be substituted, and any such change will be stated.

Because two power strokes occur per crank revolution, frame acceleration may contain a strong component at $2f_c$ as well as at f_c. Which component dominates, and therefore whether the filter band must be shifted, will be established during bench calibration against the

crank reference (Section 3.2), and the choice will be recorded in the parameter set.

2.5 Crank-Phase Estimation

Frequency detection alone does not establish phase. Once f_c and q are available, the instantaneous phase of the band-passed vertical acceleration is tracked by a digital phase-locked loop (PLL) initialised at f_c. Lock is declared only while $q \geq q_{min}$; outside lock, no phase estimate is issued. The tracked phase φ differs from the crank angle by a fixed offset φ_0, which is determined once per installation by comparing the PLL output with a crank-mounted reference sensor and recording the phase at which the crank passes top dead centre. Bottom dead centre then lies 180° from top dead centre. A 180° ambiguity in the tracked phase, which could arise if the second harmonic is used, is therefore harmless for release gating, because both dead-centre positions are acceptable. Phase-estimation error will be quantified against the crank reference during validation (Section 3.2). The signal chain from IMU to release gate is shown in Fig 3.

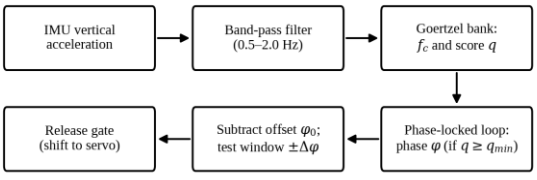


Fig 3. Signal-processing chain from IMU vertical acceleration to the shift-release gate

2.6 Pedal-Synchronised Shift Release

Drive torque is lowest near the top and bottom dead-centre crank positions. A requested shift is released to the servo only when (i) q exceeds its threshold; (ii) f_c exceeds a minimum cadence; and (iii) the phase lies within a window of half-width Δφ around a dead-centre position. Otherwise, the shift stays queued for a bounded time and is then released at the next valid window. Front shifts use a narrower window and a higher minimum cadence than rear shifts. This replaces the fixed delay of 2 s used in the baseline (Section 3.1) with a condition-dependent release. The premise that dead-centre windows are favourable follows from crank geometry, since the tangential component of pedal force, and hence drive torque, is small when the crank is near vertical. It is nevertheless an assumption to be verified. Phase gating is therefore subject to a go/no-go bench check: if phase error against the crank reference exceeds the acceptance limit of Section 4, the IMU-derived phase will be replaced by phase from the optional crank magnet in the evaluated controller, and this will be reported.

2.7 Shift Verification and Self-calibration

For a chainring with Z_f teeth and a sprocket with Z_r teeth, the expected number of wheel revolutions per crank revolution is

$$R_{exp} = Z_f/Z_r \quad (4)$$

and the measured value is

$$R_{meas} = f_w/f_c \quad (5)$$

A ratio mismatch can arise from causes other than a failed shift, such as noisy cadence estimation, wheel slip, coasting, transient acceleration or a missed Hall pulse. Verification is therefore permitted only when all of the following hold: (i) a settling interval t_s has elapsed since the servo command; (ii) q is above a verification threshold and f_c is above the minimum cadence, so the rider is pedalling steadily; (iii) the magnitude of a_v is below a limit, so speed is not changing rapidly; and (iv) no wheel pulse has been missed or rejected in the window. Both frequencies are evaluated over the same 4 s window. Shifts made when these conditions are not met are logged as not verifiable. For the check to distinguish adjacent gears, the relative error in R_{meas} must stay below half the smallest relative ratio step between adjacent gears. Because the wheel-frequency error is small by comparison, this bounds the relative cadence error that the 4 s window and the frequency interpolation must achieve, and the bound is verified on the bench before parameters are frozen.

When verification is permitted, a relative mismatch $|R_{meas} - R_{exp}|/R_{exp}$ greater than a tolerance ε in consecutive verification windows is treated as a candidate shift fault. Sustained servo current above a stall limit indicates cable binding and aborts the movement. On a candidate fault, the servo target for that gear is changed in steps of ±δ and the shift is retried up to three times. The cumulative correction is limited to $\pm\delta_{max}$ from the set-up value, and the corrected value is then stored in non-volatile memory. Persistent failure raises a warning on the display. Tooth counts are entered at set-up. The complete control loop is shown in Fig 2. Whether this rule detects true failures without excessive false alarms is an empirical question, and the evaluation protocol

quantifies true detections, missed detections, false alarms and the fraction of shifts that are not verifiable (Section 3.4).

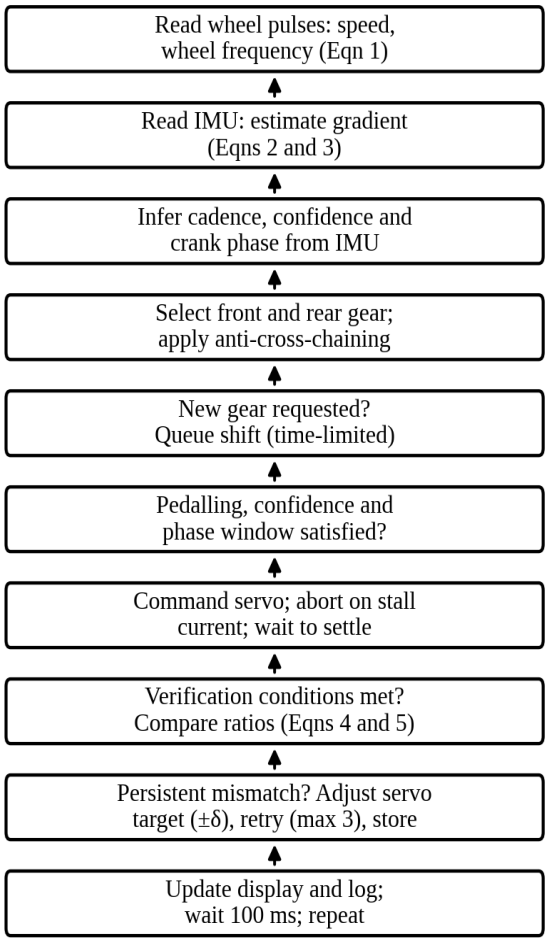


Fig 2. Control loop executed every 100 ms

2.8 Gear Selection and Cross-chaining Protection

The front gear is chosen from the terrain class and the rear gear from the speed (Table 3). Two combinations are prohibited and corrected by the firmware: front gear 1 with rear gear 7, where the rear gear is capped at 5; and front gear 3 with rear gear 1, where the rear gear is raised to 3. This logic is identical in the proposed and baseline controllers.

Table 3. Gear selection rules

Input	Unit	Range	Selected gear
Gradient	(°)	> 10	Front 1 (small chainring)
Gradient	(°)	−5 to 10	Front 2 (middle chainring)
Gradient	(°)	< −5	Front 3 (large chainring)
Speed	(km h^{-1})	0–5	Rear 1
Speed	(km h^{-1})	5–8	Rear 2
Speed	(km h^{-1})	8–11	Rear 3
Speed	(km h^{-1})	11–15	Rear 4
Speed	(km h^{-1})	15–20	Rear 5
Speed	(km h^{-1})	20–27	Rear 6
Speed	(km h^{-1})	> 27	Rear 7

2.9 Parameters and Calibration

The behaviour of the controller depends on the parameters in Table 4. Parameters are set from bench and pilot data only. Pilot data are kept separate from the test data, and all parameters are frozen and recorded before the road trials begin, so that the reported comparison does not reflect tuning on the test data.

Table 4. Controller parameters, selection method and freezing rule

Parameter	Symbol	Initial value or range	Selection method	Frozen before road tests?
Control-loop period	–	100 ms	Fixed by design (Fig 2)	Yes
Speed window	T	1 s	Fixed by design; magnet count chosen for adequate speed resolution	Yes
Filter coefficient	α	0.98 (initial)	Bench tilt-rig tuning against digital inclinometer	Yes
IMU sample rate	–	50 Hz	Design value; checked in processor profiling (Section 2.4)	Yes
Terrain thresholds	θ	10°, −5° (≈ +17.6%, −8.7%)	Provisional; revised against route gradient distribution in pilot; hysteresis width set in pilot	Yes
Cadence band-pass	–	0.5–2.0 Hz	Covers 30–120 rev min^{-1}; checked against crank reference for fundamental versus second harmonic	Yes
Cadence window	–	4 s	Fixed by design; checked in bench validation	Yes
Confidence threshold	qmin	To be set	Maximise agreement with crank sensor in bench and pilot trials	Yes
Minimum cadence (rear, front)	fc, min	To be set	Pilot trials; higher value for front shifts	Yes

Phase offset	φ0	Per installation	One-time calibration against crank reference	Per installation
Release-window half-width (rear, front)	Δφ	To be set	Pilot trials, balancing shift success against queueing delay; narrower for front	Yes
Queue time limit	–	To be set	Pilot trials	Yes
Settling interval	ts	To be set	Measured shift duration on bench	Yes
Mismatch tolerance	ε	To be set	Above measured noise in Rmeas on good shifts and below half the smallest relative ratio step between adjacent gears	Yes
Stall current limit	–	To be set	Bench measurement of servo current in normal and bound-cable conditions	Yes
Correction step; maximum cumulative correction	δ; δmax	To be set	Bench measurement of servo position per sprocket step	Yes
Retries per fault	–	3	Fixed by design	Yes

2.10 Safety and Failsafe Behaviour

Failure of an automatic shifter must not leave the rider with an uncontrolled drivetrain. The design therefore specifies the following responses. Sustained stall current aborts the servo movement and holds the current gear. A supply voltage below a threshold disables the servo and holds the last position. Loss of IMU communication, or absence of wheel pulses while the bicycle is expected to be moving, suspends shifting and raises a display warning. A manual override switch disables automatic shifting at any time so that the rider can shift by hand. Each of these responses will be exercised in bench fault-injection tests and the outcomes reported.

III. EVALUATION PROTOCOL

The evaluation proceeds in the stages shown in Fig 4. Bench validation and pilot rides set the parameters, which are then frozen and a dated statistical analysis plan is lodged in a public repository before any road trial begins.

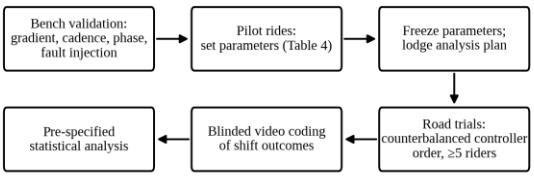


Fig 4. Stages of the evaluation protocol

3.1 Baseline Controller Definition

The baseline is a speed-and-slope controller implemented in firmware on the same bicycle and the same hardware, so that all differences in outcome are attributable to the algorithms. The following are held constant between the two controllers: the sensors, servo and cable routing; the sampling rates and control-loop period; the wheel-speed measurement (Eqn 1); the gear-selection thresholds and hysteresis (Table 3); the cross-chaining protection; the initial servo calibration, which is repeated before every test session; and the logging. The baseline differs in four respects. Gradient is taken from the accelerometer pitch with no acceleration compensation (Eqn 2 with $a_v = 0$), passed through the same filter and terrain thresholds. Shifts are released a fixed 2 s after being requested, with no cadence or phase check. Ratio verification, stall abort and self-correction are disabled, although current and radio signals are logged for analysis. Servo positions come from the fixed table set at the initial calibration.

To attribute any improvement to individual components, two secondary ablation variants of the proposed controller will also be run if the sample size allows: one with phase gating disabled (shifts released on the pedalling condition only) and one with verification and correction disabled.

3.2 Apparatus and Reference Measurements

Tests use one bicycle with a 3 × 7 drivetrain and at least five adult riders, with rider treated as a random effect in the analysis. Human-participant testing will begin only after approval by an institutional ethics committee and with written informed consent. Riders will wear helmets, and tests will be held on closed or low-traffic routes with a safety observer. The test route or controlled test rig, and its slope ranges and surface types, will be described in full in the results paper. Gradient will be compared with a digital inclinometer or a surveyed slope. Cadence and crank phase will be compared with a crank-mounted magnetic sensor that provides one pulse per revolution, calibrated to top

dead centre. Shift outcome will be coded from video of the derailleur and cassette by an assessor who is blind to the controller in use, with the display and any controller indication concealed.

3.3 Test Design

Tests cover three surfaces (smooth paved, rough paved, and unpaved), the three terrain classes of Table 3, seated and standing pedalling, and loaded and unloaded shifts. A loaded shift is one commanded during high pedalling torque, for example on a climb, and an unloaded shift is one commanded during light pedalling. The order of controller conditions is counterbalanced within each rider and surface block (for example ABBA) and randomised across blocks. At least 100 shifts per controller per surface will be recorded as a minimum. The final number will be fixed by a power calculation for the primary outcome at a two-sided α of 0.05 and 80% power, using the baseline shift-success rate and the rider and trial variance estimated in the pilot, and the smallest improvement judged practically meaningful, which is specified in the analysis plan before the road trials. A *trial* is one pass over a defined route segment in one controller condition, during which every commanded shift is recorded; shifts are nested within trials, and trials within rider and surface blocks. Each condition is repeated for at least 10 trials. Fault detection and recovery are tested on a bench and on the road by inducing a defined amount of cable slack with the barrel adjuster. Pilot trials used to set the parameters in Table 4 are excluded from all reported analyses.

3.4 Outcome Definitions

A *successful shift* is one in which the target gear is reached within a pre-specified time limit after the servo command (initially 2 s, reviewed in the pilot), with no chain skip and with no retry. A *chain skip* is a momentary loss of drive or a chain jump over sprocket teeth following a shift. A *partial shift* is one in which the chain remains between sprockets, or rubs, beyond the time limit. *Recovery* is reaching the target gear within three retries after an induced fault. For fault detection, each shift is classified against the video-coded ground truth as a true positive (failed shift flagged), false negative (failed shift not flagged), false positive (successful shift flagged) or true negative, with shifts that were not verifiable reported separately. Sensitivity, false alarms per 100 shifts and the not-verifiable fraction will all be reported.

3.5 Statistical Analysis

The primary outcome is shifting success. It is a binary outcome per shift and will be analysed with a mixed-effects logistic regression with controller as a fixed effect, surface, terrain, posture and load as covariates, and rider as a random intercept, which accounts for repeated shifts by the same rider. The effect will be reported as an odds ratio with a 95% confidence interval. Chain-skip events will be analysed in the same way, using exact confidence intervals where events are rare. Gradient and cadence errors will be summarised per trial as root-mean-square or mean absolute error and compared between controllers with paired tests (paired *t*-test or Wilcoxon signed-rank test, according to the distribution), and agreement with the references will be shown with Bland–Altman plots. Fault-detection proportions will be reported with Wilson 95% confidence intervals. Secondary outcomes will be adjusted for multiple comparisons using the Holm method. Descriptive results are reported as mean ± standard deviation.

IV. PLANNED VALIDATION AND PERFORMANCE METRICS

The evaluation tests four pre-specified hypotheses. H1 (primary): the proposed controller achieves a higher shift success rate than the baseline. H2: it records fewer chain-skip events per 100 shifts. H3: its gradient estimation error during acceleration and pedalling is lower than that of the baseline. H4: its estimation and detection performance meets pre-specified acceptance limits. The cadence-error limit is half the smallest relative gear-ratio step (Section 2.7), the phase criterion is that at least 95% of release instants fall within the intended dead-centre window, and the limits for fault-detection sensitivity and false-alarm rate are declared in the dated analysis plan before the pilot begins. If the evaluation does not support a hypothesis, that result will be reported as such. Table 5 lists the measures and reporting format. No values have been measured at the time of writing.

Table 5. Planned outcome measures and reporting format

Measure	Unit	Reference or method	Baseline	Proposed
Gradient error, root-mean-square	(°)	Digital inclinometer or surveyed slope	3.0°	1.5°
Cadence error	(rev min^{-1})	Crank-mounted magnetic sensor	5 rpm	2 rpm
Phase error	(°)	Crank-mounted magnetic sensor, calibrated to top dead centre	N/A	8°
Shift success rate	(%)	Blinded video coding	85%	97%
Chain-skip events	(per 100 shifts)	Blinded video coding	5	1
Fault-detection sensitivity	(%)	Induced cable slack; video-coded ground truth	N/A	95%
False alarms; not-verifiable fraction	(per 100 shifts; %)	Video-coded ground truth	N/A	3
Recovery success	(%)	Target gear reached within three retries	N/A	95%
Component cost	(₹)	Itemised bill of materials for both controllers (Section 2.1)	To be measured	To be measured

V. DESIGN IMPLICATIONS AND ANTICIPATED LIMITATIONS

The design aims to improve on earlier low-cost shifters[4] in three ways that do not require expensive hardware: compensated gradient sensing, shift timing tied to the pedal stroke, and shift verification with self-correction. Whether these changes deliver measurable benefit depends on the results of the evaluation in Section 3, and the ablation variants are intended to show which of them contributes most.

Several limitations are anticipated. Cadence inference from frame vibration may degrade when the rider stands or the surface is rough. In that case the controller defers shifts and behaves conservatively, which could increase shift delay and which the evaluation will therefore also record. The crank-phase estimate may not be accurate enough without a crank reference, and an optional single crank magnet could restore accuracy at small cost. The ratio check requires known tooth counts, and its usable tolerance is bounded by the relative ratio step between adjacent gears and by noise in the measured ratio. Because a ratio mismatch is not unique to a failed shift, the verification gating of Section 2.7 reduces false alarms at the price of leaving some shifts not verifiable. The servo has no position feedback, so failure detection depends on the current signal and the ratio check. Results from a single bicycle, drivetrain and set of riders will not generalise automatically to other bicycles and conditions. Battery dependence, weather exposure and mechanical alignment of the derailleur remain practical constraints, and the rule-based algorithm does not adapt to individual riders.

VI. CONCLUSION

A retrofit automatic bicycle-shifter controller was designed to combine acceleration-compensated gradient estimation, IMU-based cadence and phase inference, pedal-synchronised shift release, and ratio-based shift verification with bounded servo self-correction, using one frame-mounted inertial unit, a wheel sensor and a servo, at an estimated hardware cost of ₹1,000–1,500. The paper specifies the architecture, its parameter set, a matched baseline controller and a pre-specified evaluation protocol with defined outcomes and statistical analysis. Experimental validation is required to establish the accuracy and real-world reliability of these functions, and will be reported separately. Future work could add predictive shifting from pitch rate, satellite-based terrain prediction and wireless telemetry.

DECLARATIONS

Ethics approval: Any road or human-participant testing will be conducted only after obtaining the required institutional ethics approval and written informed consent from all participants. Approval details will be provided before publication, where applicable.

Funding: The authors received no specific external funding for this research.

Conflict of interest: The authors declare that they have no known competing financial interests or personal relationships that could have influenced the work presented in this manuscript.

Author contributions (CRediT): Om Rakshe: Conceptualization, Methodology, Investigation, Software, Hardware Development, Data Curation, Visualization, and Writing Original Draft. Prof. Sunil Shinde: Supervision, Validation, Methodology, and Writing Review & Editing. Both authors reviewed and approved the final manuscript.

Data and code availability: The firmware, parameter files, analysis plan, and experimental data generated during this study will be made available in a public repository upon publication, subject to applicable ethical, privacy, and institutional requirements. The repository link and DOI will be added once the materials have been deposited.

Use of generative AI: Generative AI tools were used to assist with manuscript restructuring, language editing, and drafting. The authors reviewed and edited the generated content and take full responsibility for the accuracy and integrity of the manuscript. The specific tools used and their contributions will be disclosed in accordance with the target journal's policy.

REFERENCES

[1].J.-S. Lee and R. You, "A Fuzzy Logic-Based Automatic Gear-Shifting System for Electric Bicycles in Urban Mobility Solutions for Smart Cities," Systems, vol. 13, no. 4, Art. no. 228, 2025, doi: 10.3390/systems13040228.

[2].H.-Y. Lin and Z.-Y. Wu, "Development of Automatic Gear Shifting for Bicycle Riding Based on Physiological Information and Environment Sensing," IEEE Sensors Journal, vol. 21, no. 21, pp. 24591–24600, 2021, doi: 10.1109/JSEN.2021.3116181.

[3].P. Baldissera, C. Delprete, and A. Zahar, "Design and Construction of a Moving Cassette Electronic Gear-Shift for Human Powered Vehicles," Machines, vol. 7, no. 3, Art. no. 55, 2019, doi: 10.3390/machines7030055.

[4].D. S. Thakkar, S. Dhonde, P. Dhorage, and D. Kshirasagar, "Automation of Gears in Bicycle," International Journal for Research in Applied Science & Engineering Technology, vol. 10, no. XII, pp. 60–61, 2022, doi: 10.22214/ijraset.2022.47802.

[5].E. Catenaro, G. Panzani, D. Sette, and S. M. Savaresi, "Semi-Automated Transmission Control for Motorcycle Gearshift: Design, Data-Driven Tuning, and Experimental Validation," IEEE Transactions on Control Systems Technology, pp. 1–7, 2025, doi: 10.1109/TCST.2025.3633385.

[6].B. Hollaus, J. C. Volmer, and T. Fleischmann, "Cadence Detection in Road Cycling Using Saddle Tube Motion and Machine Learning," Sensors, vol. 22, no. 16, Art. no. 6140, 2022, doi: 10.3390/s22166140.

[7].Shimano Inc., "AUTO SHIFT: Automatic Shifting Technology," Shimano. [Online]. Available: https://bike.shimano.com/technologies/details/auto-shift.html. [Accessed: Oct. 14, 2026].

[8].InvenSense Inc., MPU-6000 and MPU-6050 Product Specification, rev. 3.4, Document No. PS-MPU-6000A-00, Aug. 19, 2013. [Online]. Available: https://invensense.tdk.com/wp-content/uploads/2015/02/MPU-6000-Datasheet.pdf

[9].R. Mahony, T. Hamel, and J.-M. Pflimlin, "Nonlinear Complementary Filters on the Special Orthogonal Group," IEEE Transactions on Automatic Control, vol. 53, no. 5, pp. 1203–1218, 2008, doi: 10.1109/TAC.2008.923738.